Investigation of Ring-Type Ion Ventilator

I. Andrijauskas[1], V. Siozinys[1], S. Zebrauskas[1]
[1]*Department of Electric Power Systems, Kaunas University of Technology, Studentu St. 48–210, LT-51368 Kaunas, Lithuania*
vytautas.siozinys@ktu.lt

***Abstract*—A prototype of ionic wind fan is presented. Modelling using numerical methods was performed. The physical model was created. The calculated theoretical results were compared with measurement results in physical model. Overall efficiency of the system was calculated. Digital simulation model was created using "COMSOL Multiphysics". The air flow measurement uncertainties due to instrumentation were discussed. The air flow model in tube was investigated and airflow measurement incarnates were removed.**

***Index Terms*—Ion, ventilator, gas flow.**

I. Introduction

Ion-driven gas flows have many advantages to conventional fans or blowers. For example, ion-driven or electrohydrodynamic (EHD) flow requires no moving parts and provides flexibility in duct shape since the cross-section of the duct is unconstrained [1].

Ionic wind fans are discussed in [2]. In example [2] needle to grid electrode systems are used. The experiment was carried out at high electric field strength values, and a relatively high wind speed was achieved. In our case, we used a different geometry of the electrode system – needle – ring. Obtained ionic wind power compared to the electric power consumed.

Also thermo-anemometer sensor affect to the measurement results is found. View of the fact the correction factor is found, which allows the laboratory to find out the actual speed.

II. Model of Prototype

This study aims to verify needle – ring system similar to the system mentioned in the literature [2]. The model of a prototype created for experiment is shown in Fig 1. It shows the copper needle and a ring, distance *a* is variable. In the experiment described in [2], the wind speed was measured at 2 cm from the end of the pipe. In the end of a pipe the grid was established. In this study, the electrode system is placed in the centre of a PVC cylinder of 30 cm length, to ensure the quality of the measurement results and a continuous flow.

III. Modelling of Electric Field

The dashed rectangle (Fig. 1) indicates the electric field region, which is calculated using the finite element method of COMSOL Multiphysics software package.

Manuscript received January 13, 2014; accepted April 21, 2014.

Electric field between the needle and the ring is modelled using COMSOL Multiphysics software.

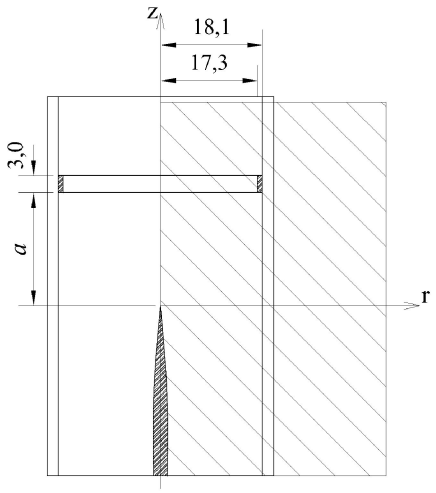

Fig. 1. Model of a prototype and a field of calculations with boundaries.

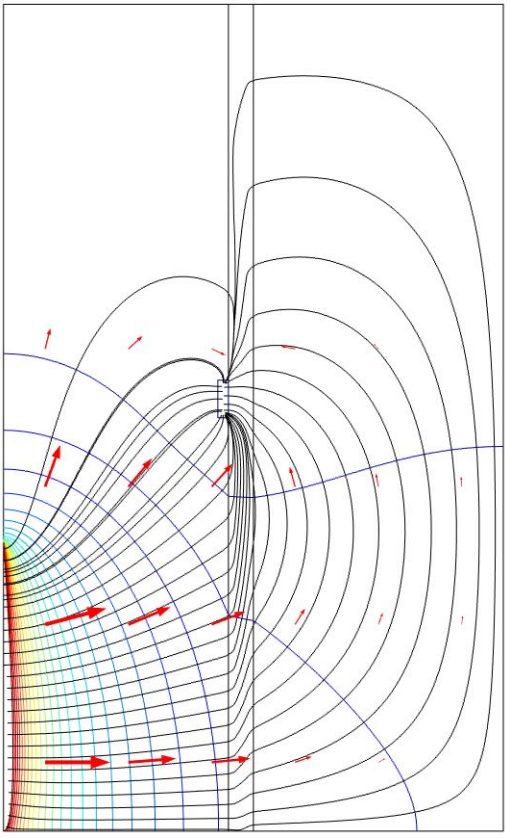

Fig. 2. Electric field. equipotential lines differing by 500 V step and field lines at a distance a = 10 mm and the needle electrode voltage U = 12 kV.

Both the modelling of the electric field, as well as the measurements were chosen for the voltage range from U_0 = 5 kV to 12 kV with ΔU = 1 kV increments, and two values of distance a = 10 mm and a = 20 mm. Other settings such as the ring diameter, thickness, width, needle shape, pipe wall thickness were constant. System of DC corona discharge equations was used for modelling of the field:

$$\nabla \cdot \mathbf{D} = \rho_V, \quad (1)$$

$$\mathbf{E} = -\nabla V, \quad (2)$$

$$W = \int_{V'} \frac{qU}{2} \mathrm{d}V', \quad (3)$$

$$q = \oint_A \mathbf{D} \mathrm{d}\mathbf{A}, \quad (4)$$

where D is electric flux density vector, ρV' is volume density of space charge, E is electric field strength vector, V is potential, V' is volume, W is energy, q is electric charge, U is voltage, A is surface area and dA is area element vector.

Equipotential and field lines of digital simulation field model at a distance a = 10 mm are shown in Fig. 2.

Corresponding lines of digital simulation field model at a distance a = 20 mm are shown in Fig. 3.

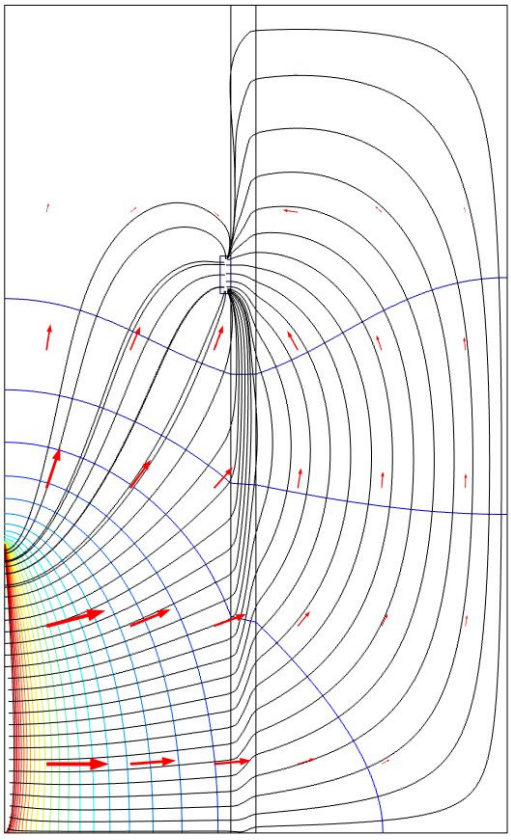

Fig. 3. Electric field. equipotential lines differing by 500 V step and field lines at a distance a = 20 mm and the needle electrode voltage U = 12 kV.

After digital simulation of the electric field in the needle – ring electrode system theoretical device power is received by multiplying the energy density by the volume of the cylinder. Comparison of this value P_{comsol} with the measured power P_{electric} is presented in Fig. 7.

Analysing the character of field lines shown in Fig. 2 and Fig. 3 it can be seen that part of the field-strength lines curl the ring thus creating turbulence.

IV. Experiment of Wind Speed Measuring

To get a corona discharge a needle with high potential, a grounded ring, PVC pipe and a high-voltage source are needed (Fig. 1). The distance a between the needle and a ring is variable, the ring inner radius is 17.3 mm and ring thickness is 1 mm. Experiment and model was taken at a distance of a = 10 mm and 20 mm from the tip of the needle to the bottom of the ring. In this context it does not matter whether the needle charge is positive or negative ionic wind still blowing from the needle toward the ring. The current I is measured between the grounded electrode and the ground. The aim is to analyse the ionic wind at the end of the pipe. The starting point of coordinate corresponds to the needle tip. Wind speed was measured by the anemometer sensor at the end of the pipe so that the sensor can measure the wind in the z direction (Fig. 1). During the test the temperature in the room was 21 °C.

We use thermo-anemometer Delta OHM DO9847 and sensor AP471S1 for wind speed measurement, the scheme of sensor is presented in Fig. 4.

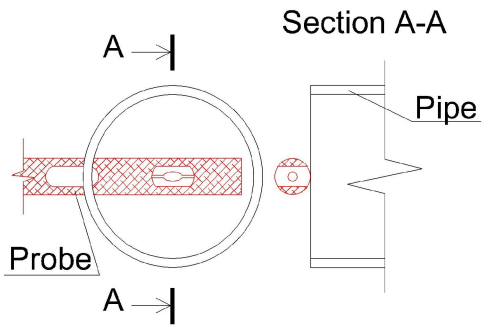

Fig. 4. Measuring device sensor diagram.

The experiment results of relationship between maximum wind speed measured inside pipe and power consumption is shown in Fig. 5.

Current-voltage characteristics of system are shown in Fig. 6.

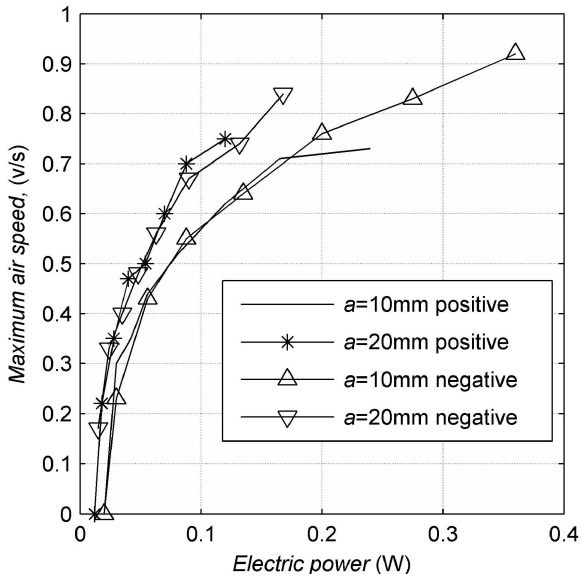

Fig. 5. The maximum wind speed dependence on electric power consumption.

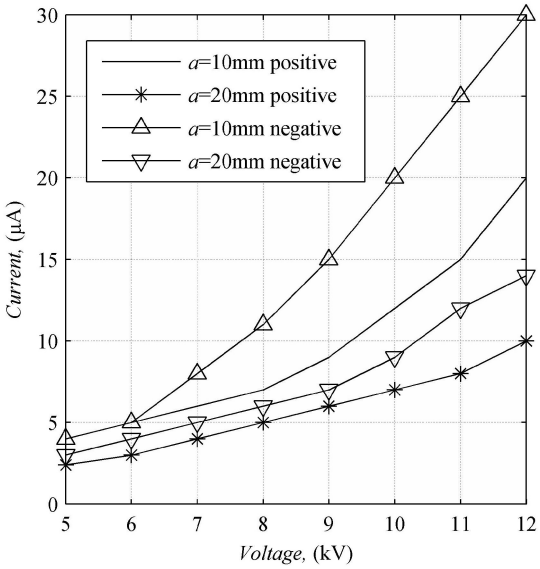

Fig. 6. Current-voltage characteristic of system.

It can be seen from the measurement results (Fig. 5 and Fig. 6) that if the distance between the needle electrode and the ring is 10 mm and discharge is positive, ionization process begins at 6 kV, while at a negative discharge (negative electrode) the phenomenon of ionization begins at 9 kV. Increasing the distance between the electrodes up to 20 mm, the electric field strength between the needle and ring is reduced resulting that ionisation process is weakened and begins at 9 kV÷10 kV in the case of negative discharge and reaches 11 kV for positive discharge.

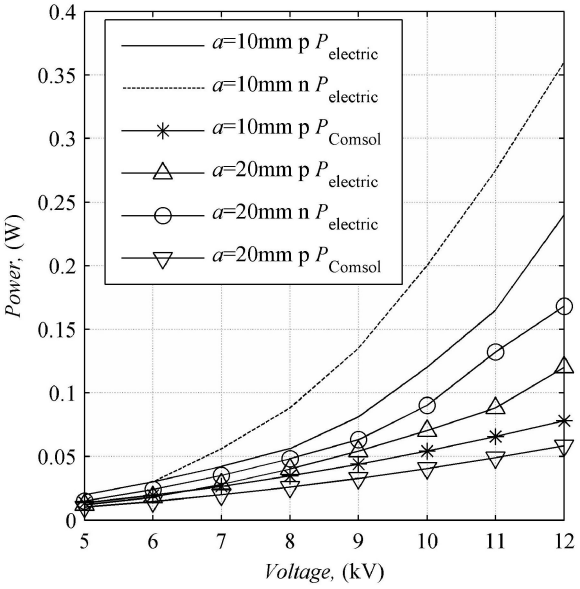

Fig. 7. Comparison of measured electrical power with the simulation results.

While on the one hand the phenomenon of ionization creates intense charges movement - ionic wind, but as shown in Fig. 5 enhanced ionization process only increases energy consumption but does not increase in proportion to the wind speed due to beginning of saturation.

As can be seen from the electric field strength of the modelling results in Fig. 2 and Fig. 3, the electric field lines curl the ring, thus creating turbulence in mass transfer. Although the ionization process enhanced at a distance of 10 mm, but the electric field unevenness, higher wind speed is not achieved compared to the 20 mm design.

V. MEASURING DEVICES INFLUENCE ON MEASUREMENTS

As shown in Fig. 4 dimensions of thermo-anemometer sensor AP471S1 are quite significant in comparison to the cylinder diameter. Laminar flow hydraulic problem was modelled in order to determine the measurement error.

To calculate laminar flow tasks “COMSOL Multiphysics” uses Navier-Stokes equation (5)

$$\circ \frac{\partial u}{\partial t} + \circ (u \cdot \nabla) u = $$
$$= \nabla \left[-p\mathbf{I} + « \left(\nabla u + (\nabla u)^T \right) - \frac{2}{3} « (\nabla u)\mathbf{I} \right] + F, \qquad (5)$$

where « is dynamic viscosity, Pa·s, u is the speed, m/s, $\circ$ – density, kg/m^3, p – pressure, Pa, T – component of the total stress tensor, I – identity matrix 3x3, F – body forces, N.

Laminar flow rate was set at v_0 = 0,5 m/s, as can be seen from Fig. 8 wind speeds of up to v_{max} = 0,7096 m/s. This rate if compared with that established is large enough to reduction of impact was calculated correction factor. The evaluation of the average rate of the three sections in the direction of z at coordinates 100, 105 and 110 with the sensor and in the same cross-sections without the sensor.

More accurate maximum wind speed $v_{\max,k}$, when the largest measured is sensor velocity known as $v_{\max,measured}$

$$v_{\max,k} = \frac{v_{\max,measured}}{k}. \qquad (6)$$

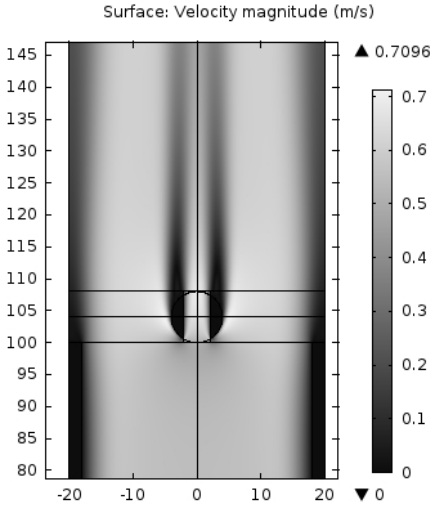

Fig. 8. Air mass velocity profile is influenced by the measuring device.

Correction factor value calculated to eliminate sensor caused error is k = 0,924.

It is assumed that the mean velocity profile is a half of the maximum wind speed in the centre.

The average wind speed in the pipe depends on the distance between the electrodes, electrode voltage and polarity. The dependences are shown in Fig. 9.

VI. OVERALL SYSTEM EFFICIENCY

Assuming that the flow is laminar, average speed calculated over the cross section is the following

$$Q = Av, \tag{7}$$

where A is cross section area, m^2, v is average speed, m/s.

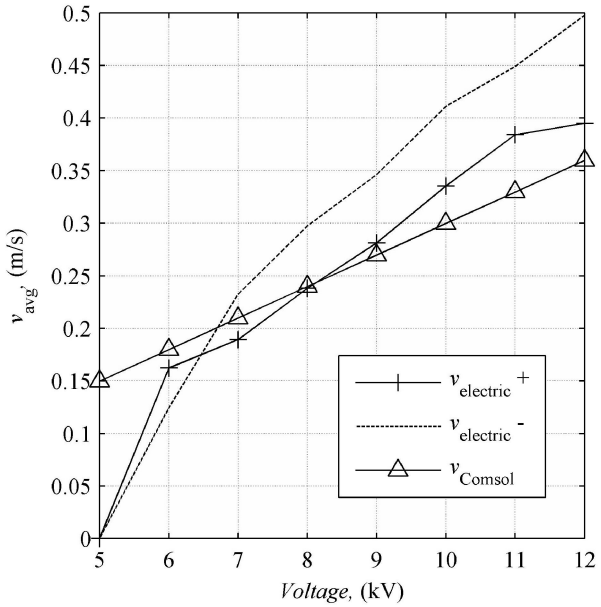

Fig. 9. The measured and calculated wind speed dependence on the voltage at a = 10 mm and at a = 20 mm.

If the flow rate and the average speed of flowing air is a known mechanical power, it is calculated as follows [3]

$$P_{\text{mech}} = \frac{\rho Q v^2}{2}, \tag{8}$$

where ρ – density, kg/m^3, v – average speed, m/s.

The rate of electric energy consumption is calculated from

$$P_{\text{electric}} = UI. \tag{9}$$

Efficiency of the ion fan can be calculated by using the mechanical (8) and electrical (9) power

$$\eta = \frac{P_{\text{mech}}}{P_{\text{electric}}}. \tag{10}$$

Electromechanical system efficiency depends on the distance between the electrodes and electrode voltage. The dependence is shown in Table I.

TABLE I. ELECTROMECHANICAL EFFICIENCY.

Voltage, kV			5	6	7	8	9	10	11	12
Electromechanical efficiency η, %	P	a=10mm	0.00	0.05	0.05	0.06	0.06	0.06	0.05	0.04
		a=20mm	0.00	0.05	0.08	0.10	0.08	0.09	0.10	0.08
	N	a=10mm	0.00	0.03	0.06	0.06	0.05	0.05	0.04	0.04
		a=20mm	0.03	0.08	0.08	0.09	0.09	0.09	0.07	0.08

The maximum efficiency is achieved when a distance between needle and ring is 20 mm, whether positive and negative needle polarity. Experiment results compared to the results [2] lead to the conclusion that the mesh electrode configuration increases system efficiency compared with the ring electrode configuration.

As mentioned in [4] system would use less power and be more efficient with smaller radius of the needle top.

VII. CONCLUSIONS

Recommended electric field strength direction should be as much as possible parallel to the air flow direction.

Investigation has revealed that for defined electrode configuration the overall system efficiency increase with increase of distance between electrodes.

The meshed ground electrode configuration has bigger mechanical efficient than the ring ground electrode configuration.

Mechanical efficiency of 0.1 % was reached for the ring electrode configuration.

REFERENCES

[1] M. Rickard, D. Dunn-Rankin, "Numerical simulation of a tubular ion-driven wind generator", *Journal of Electrostatics*, vol. 65, pp. 646–654, 2007. [Online]. Available: http://dx.doi.org/10.1016/j.elstat.2007.04.003

[2] E. Moreau, G. Touchard, "Enhancing the mechanical efficiency of electric wind in corona discharges", *Journal of Electrostatics*, vol. 66, pp. 39–44, 2007. [Online]. Available: http://dx.doi.org/10.1016/j.elstat.2007.08.006

[3] E. Moreau, "Airflow control by non thermal plasma actuators", *J. Phys. D: Appl. Phys.*, vol. 40, pp. 605–636, 2007. [Online]. Available: http://dx.doi.org/10.1088/0022-3727/40/3/S01

[4] I. Andrijauskas, S. Zebrauskas, "Analysis of an electrostatic field in electrode system of devices for drying of powdery materials", *Electrical and Control Technologies*, pp. 117–120, 2013.